Amphiphilic guanidinocalixarenes inhibit lipopolysaccharide (LPS)- and lectin-stimulated Toll-like Receptor 4 (TLR4) signaling

Stefania E. Sestito[a], Fabio A. Facchini[a], Ilaria Morbioli[b], Jean-Marc Billod[c], Sonsoles Martin-Santamaria[c], Alessandro Casnati[b], Francesco Sansone[b]* and Francesco Peri[a]*

[a]Department of Biotechnology and Biosciences, University of Milano-Bicocca, Piazza della Scienza, 2; 20126 Milano (Italy).

[b]Dipartimento di Scienze Chimiche, della Vita e della Sostenibilità Ambientale, Parco Area delle Scienze 17/a, 43124 Parma

[c]Department of Chemical & Physical Biology, Centro de Investigaciones Biologicas, CIB-CSIC. C/ Ramiro de Maeztu, 9. 28040-Madrid (Spain).

Abstract: We recently reported on the activity of cationic amphiphiles in inhibiting TLR4 activation and subsequent production of inflammatory cytokines in cells and in animal models. Starting from the assumption that opportunely designed cationic amphiphiles can behave as CD14/MD-2 ligands and therefore modulate the TLR4 signaling, we present here a panel of amphiphilic guanidinocalixarenes whose structure was computationally optimized to dock into MD-2 and CD14 binding sites. Some of these calixarenes were active in inhibiting, in a dose-dependent way, the LPS-stimulated TLR4 activation and TLR4-dependent cytokine production in human and mouse cells. Moreover, guanidinocalixarenes also inhibited TLR4 signaling when TLR4 was activated by a non-LPS stimulus, the plant lectin PHA. While the activity of guanidinocalixarenes in inhibiting LPS toxic action has previously been related to their capacity to bind LPS, we suggest a direct antagonist effect of calixarenes on TLR4/MD-2 dimerization, pointing at the calixarene moiety as a potential scaffold for the development of new TLR4-directed therapeutics.

Introduction

The members of the Toll-like Receptor (TLR) family are among the first receptors to be activated during many host-pathogen interactions. They are responsible for detecting microbial products and inducing innate and adaptive immune responses.[1] TLRs are pattern recognition receptors (PRR) that recognize pathogen-associated molecular patterns (PAMPs). Among TLRs, TLR4 is the sensor of Gram-negative bacteria endotoxins lipopolysaccharide (LPS) and lipooligosaccharide (LOS).[2] TLR4 is mainly expressed on monocytes, dendritic cells (DCs) and macrophages (MΦs). LPS binds sequentially to lipid binding protein (LBP), cluster of differentiation 14 (CD14, GPI-linked or soluble), and finally to myeloid differentiation factor 2 (MD-2)[3] that non-covalently associates with TLR4 promoting the formation of the activated receptor multimer $(TLR4/MD\text{-}2{\cdot}LPS)_2$ on the plasma membrane.[4] While the role of TLR4 as LPS sensor is fundamental for initiating inflammatory and immune responses, excessive and deregulated TLR4 activation leads to acute sepsis and septic shock, syndromes associated to high lethality for which no specific pharmacological treatment is available[5, 6]. TLR4 can also be activated by endogenous factors called damage-associated molecular patterns (DAMPs), derived from damaged, necrotic, or infected tissues. DAMPs-activated TLR4 signaling has been implicated in a large array of pathologies including atherosclerosis,[7] rheumathoid arthritis,[8] neuroinflammations, neuropathic pain,[9] and neurodegenerative diseases such as amyotrophic lateral sclerosis (ALS).[10]

To block abnormal TLR4 signaling in bacterial sepsis, two different strategies have been developed. The first one is based on LPS neutralization by the formation of non-covalent adducts with cationic compounds: positively charged antimicrobial peptides (AMP)[11] including polymixin B,[12] and synthetic dendrimeric polyamines[13, 14] contain positively charged groups (most frequently amino and guanidinium groups) and form non-covalent complexes with negatively charged LPS, thus preventing LPS to interact with the receptors.

The second strategy is based on the use of molecules that compete with endotoxic LPS in binding to the same site on CD14 and MD-2, thereby inhibiting the induction of signal transduction by

impairing LPS-initiated receptor dimerization. To date, several Lipid A variants, that specifically block the LPS-binding site on human (h)MD-2, have been identified: natural compounds such as lipid IVa (a biosynthetic precursor of *E. coli* Lipid A)[15] and a nonpathogenic Lipid A from *R. sphaeroides*,[16] and synthetic molecules as the tetraacylated disaccharide Eritoran (E5564),[17, 18] the aminoalkyl glucosaminide 4-phosphates (AGPs),[19, 20] and some phosphorylated monosaccharide glycolipids.[21] These compounds inhibit TLR4 signaling by accommodating into the deep hydrophobic pocket of the co-receptor, MD-2, and blocking ligand-induced dimerization.[22] Eritoran[23] and other small molecules with TLR4 antagonist activity[24] also potently inhibit LPS binding to CD14. While the use of LPS neutralizing agents is limited to sepsis and septic shock, TLR4 antagonists that directly bind CD14 and MD-2 have potential also as therapeutics to treat neuroinflammations[25] and viral syndromes[26] caused by DAMP-TLR4 signaling. We recently observed that glycoamphiphiles with a sugar core (trehalose or glucose) functionalized with lipid chains and positively charged ammonium groups are able to inhibit LPS-stimulated TLR4 signal in vitro with IC_{50} values ranging from about 5 to 0.2 μM and to reduce TLR4-dependent production of inflammatory cytokines in vivo.[27] The main structural feature of these molecules is their "facial" arrangement with positive charges and lipophilic chains disposed in spatially well-defined regions. Therefore, we hypothesized that calixarene-based facial amphiphiles could also be suitable as scaffolds to obtain TLR4 ligands with antagonist activity. Interestingly, amphiphile calixarenes showed remarkable properties also in a biological context significantly related to this feature.[28] The calixarene scaffold represents a very versatile structure to build amphiphilic compounds due to the possibility to variably and selectively functionalize both its upper (aromatic *para* positions) and lower (phenolic oxygens) rims. Moreover, the possibility to link to the macrocyclic platform several binding moieties, resulting in pre-organized arrays, gives rise to systems that, exploiting a multivalent effect, frequently show improved biological activity with respect to corresponding monovalent models.[28, 29] From this point of view, also the tight compaction of hydrophobic chains

located at one of the rims can result in the enhancement of some properties such as (self)assembling capabilities in an aqueous environment. [28-31]

We present here a study on the inhibition of TLR4/MD-2 signaling by a series of positively and negatively charged calixarene-based amphiphiles (compounds **1**-**6** and **7**-**9** in Figure 1, respectively) and the investigation of their mechanism of action. In the series we included calixarene **2** as reference compound whose activity in this biological context has been previously reported[32] and associated to its capacity to bind and neutralize LPS as topomimetic of LPS-binding peptides. Since we hypothesized that calixarene derivatives could directly bind to human and murine MD-2 and CD14 in a similar fashion than LPS, we preliminarily performed docking calculations to support this mode of interaction. Moreover, we aimed here to verify if the TLR4 antagonist activity is a rather general property of positively charged amphiphilic calixarenes, and if the antagonist effect also derives from the direct interaction of calixarenes with the receptors, and not exclusively from LPS neutralizing action, as suggested for calixarene **2**.

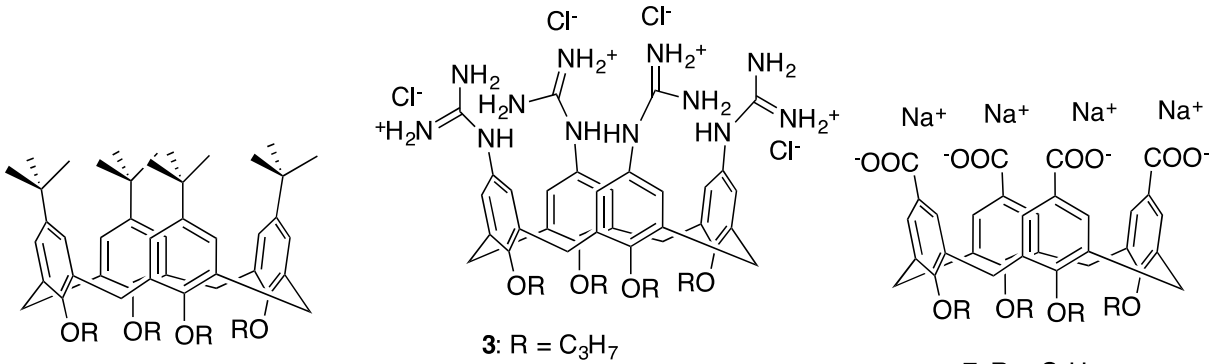

1: R = -$CH_2CH_2CH_2$-NH-C(NH_2)=NH_2^+ Cl^-
2: R = -$CH_2CH_2CH_2CH_2$-NH-C(NH_2)=$NH_2^+Cl^-$

3: R = C_3H_7
4: R = C_6H_{13}
5: R = C_8H_{17}
6: R = -CH_2CH_2-O-CH_2CH_3

7: R = C_6H_{13}
8: R = C_8H_{17}
9: R = $C_{12}H_{23}$

Figure 1. Positively charged guanidinocalixarenes **1**-**6**, and negatively charged carboxyl calixarenes **7**-**9**.

Results

Rational design of amphiphilic calixarenes as CD14/MD-2 ligands

We were inspired by the hypothesis that the calixarenes could be TLR4 modulators similarly to lipid A variants and to trehalose or glucose-based glycoamphiphiles previously developed by one of

the groups involved in the present study.[27] Positively charged guanidinocalix[4]arenes **1** and **3**-**6** and negatively charged carboxylate calixarenes **7**-**9** were designed in order to investigate the suitability of this macrocyclic scaffold to build CD14 and TLR4/MD-2 ligands (Figure 2). These calixarene derivatives have an amphiphilic character due to the presence of lipophilic tails on one rim and charged polar groups on the other. Only compound **6**, having ethoxyethyl chains at the lower rim, has a reduced amphiphilicity and was included in the library precisely to verify the possible relevance of this property in the biological activity.

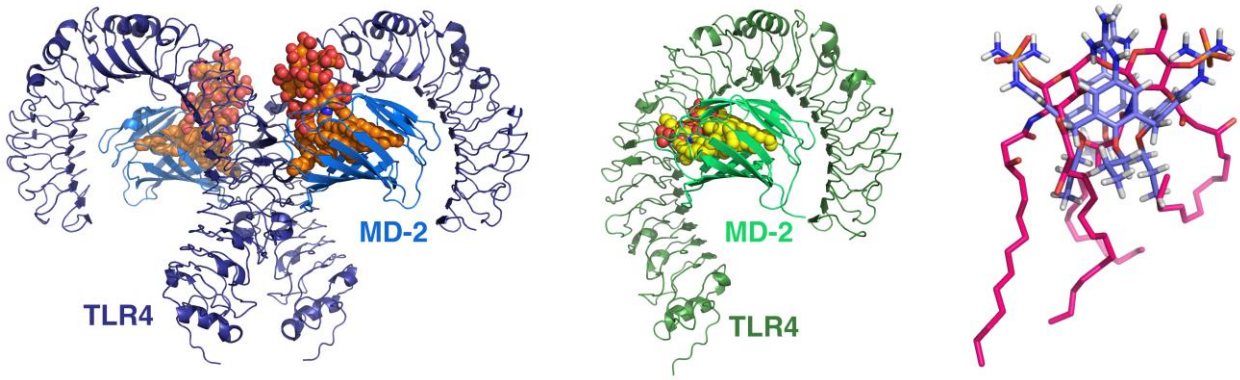

Figure 2. Left: 3D structure of human TLR4/MD-2/LPS dimer from PDB ID 3FXI. Middle: 3D structure of TLR4/MD-2/Lipid-IVa from PDB ID 2E56. Right: Superimposition of lipid IVa (from PDB ID 2E56, magenta) and calixarene **3** (purple).

Calixarenes **1** and **2**[32] present lipophilic upper rims bearing four *tert*-butyl groups and polar lower rims with positively charged guanidinium groups linked through, respectively, propyl or butyl chains. Calixarenes **3**-**6** present a reversed arrangement of lipophilic and charged groups: guanidinium groups are directly linked to the scaffold on the upper rim and hydrocarbon chains of different length (C_3, C_6 or C_8 for compounds **3**, **4** and **5**, respectively), or an ethoxy ethyl chain in the case of compound **6**, are linked at the lower rim. Finally, anionic calixarenes **7**-**9** were designed with the purpose of studying the influence of negatively charged groups. Thus, these anionic calixarenes present carboxylate groups at the upper rim, aiming to mimic the phosphate groups of LPS, and hydrocarbon chains of variable length (C_6, C_8 and C_{12}) at the lower rim.

Three-dimensional (3D) structures of compounds **1**-**9** were built and optimized by means of computational techniques (see Experimental Section). We superimposed the 3D structures of the calixarenes **2** and **3** with that of lipid IVa, a natural underacylated MD-2 ligand with activity as (h)TLR4 antagonist. When comparing lipid IVa (3D structure from the X-ray crystallography structure) with compound **3** (Figure 2-right), the oppositely charged groups (phosphate *vs* guanidinium) aligned perfectly, and also did the disaccharide over the aromatic calix backbones, and the acyl over the alkoxy chains. This preliminary result regarding the geometrical similarity prompted us to further study calixarenes **1**-**9** as putative TLR4/MD-2 and CD14 ligands.

Firstly, compounds **2**, **3** and **4**, as representative derivatives, were docked into the binding site of the human CD14 protein (PDB ID 4GLP). For all these three compounds, docking calculations predicted favorable binding poses inside the human CD14 protein (Figure 3), where the guanidinium moieties are placed at the rim of CD14 and the hydrophobic chains are inserted into the hydrophobic pocket.

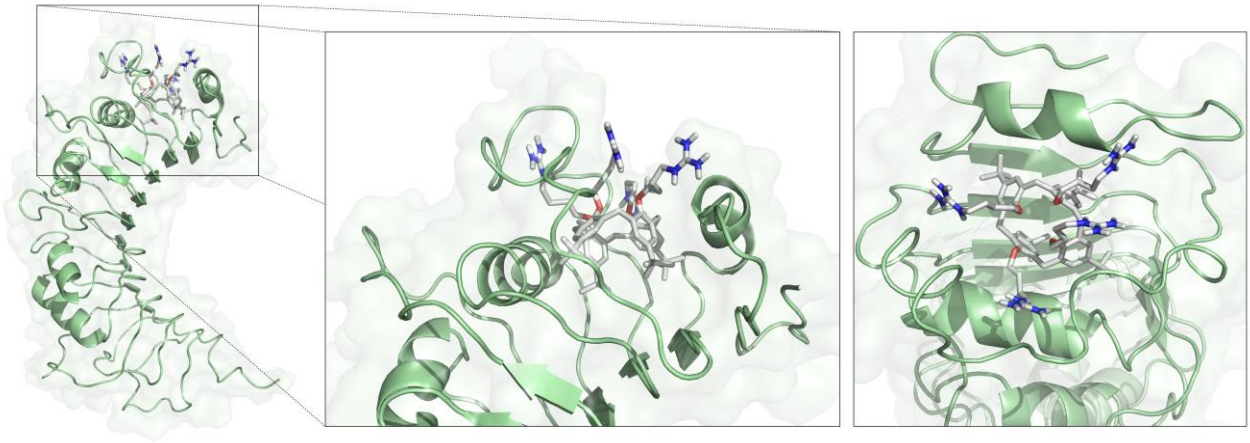

Figure 3. Docked pose for compound **3** inside CD14 (PDB ID 4GLP). Left: full perspective. Middle: side view. Right: top view.

Docking calculations were also performed with compounds **1-9** into four different structures of the TLR4/MD-2 system: human and mouse, in agonist and antagonist conformations of MD-2 (see Figures 4, and 5, and S1, S2 and S3 at Supp. Info.). Overall, all the ligands were predicted to bind inside the different TLR4/MD-2 structures, with the guanidinium/carboxyl moieties placed at the

rim of MD-2, where polar interactions predominate, and the lipophilic groups (alkoxy or *t*-butyl chains) inside the MD-2 pocket. These docked poses are in agreement with calculations reported by us of compounds binding both CD14 and MD-2 proteins. Although MD-2 is more specific in the ligand recognition, both MD-2 and CD14 binding pockets share some similarities regarding volume and accessible surface area.[33, 34]

Regarding reported compound **2**, in the docked poses in both agonist and antagonist conformations of human MD-2, the guanidinium groups establish H-bonds with the side chains of Glu92, Tyr102, and Ser118, and the backbone of Lys122 (Figures 4, S1and S2 at Supp. Info.), while one of the aromatic rings of the macrocycle is engaged in a π-π-stacking interaction with Phe119 side chain.

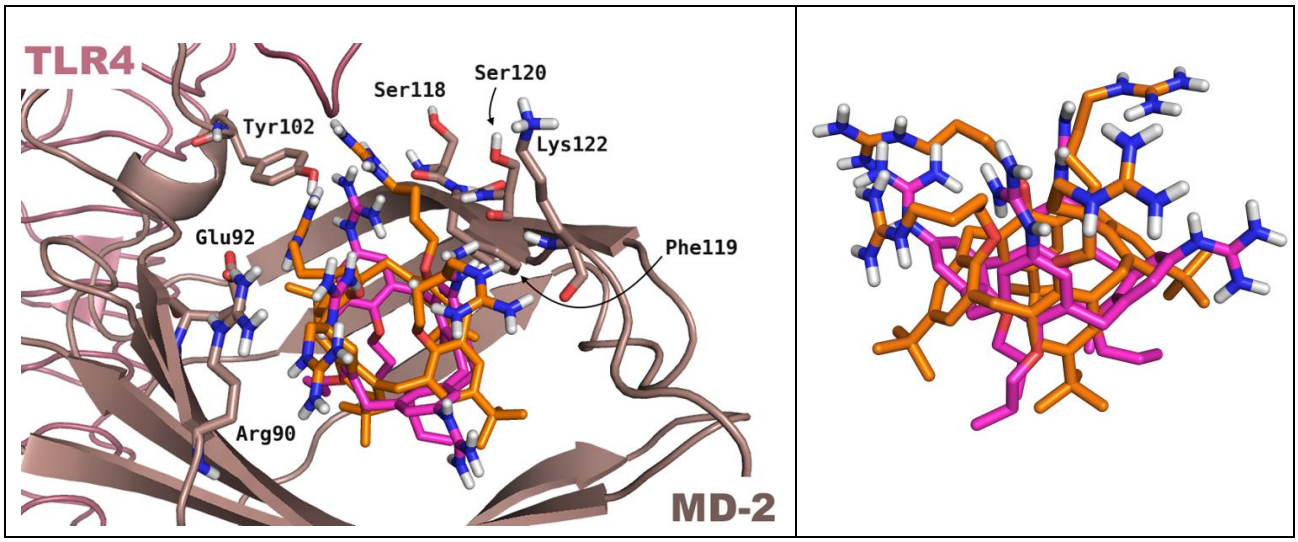

Figure 4. Superimposition of the best docked poses for compound **2** (orange) and **3** (magenta) in TLR4/MD-2 heterodimer (PDB ID 2Z65). A 90^{o} rotated view is shown on the right (TLR4/MD-2 has been hidden for the sake of clarity).

In details, the guanidinium groups at the upper rim of compounds **3**-**5** establish H-bonds with the backbone of Ser120, and the side chains of Glu92 and Tyr102 (Figure 5). The longer alkyl chains of compounds **4** and **5** occupy deeper regions of the MD-2 pocket. Interestingly, when comparing the

best predicted docked poses for compounds **2** and **3**, it was observed that they are half turn rotated one from another in regards to the calixarene moiety (Figures 4 and S2, Supp. Info.). In both cases, the guanidinium moieties are accommodated at the entrance of the pocket while the hydrophobic groups (*tert*-butyl and propyl for compound **2** and **3**, respectively) are buried inside the MD-2 hydrophobic pocket.

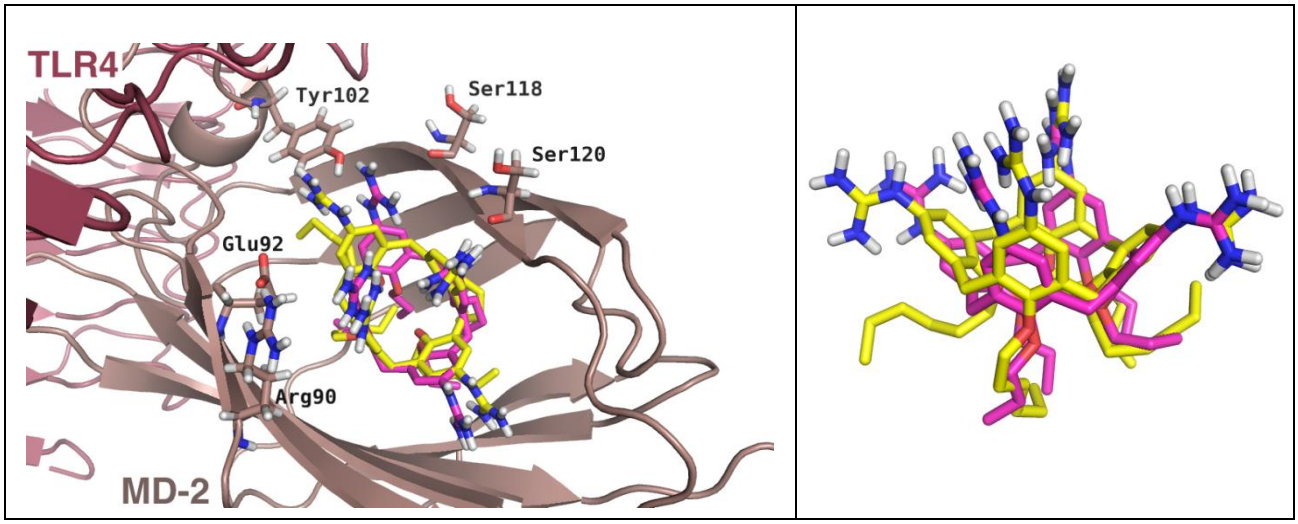

Figure 5. Superimposition of the best docked poses for compounds **3** (magenta) and **4** (yellow) in (h)TLR4/MD-2 heterodimer (PDB ID 2Z65). A 90^{o} rotated view is shown on the right (TLR4/MD-2 has been hidden for the sake of clarity).

Regarding compounds **7**-**9**, they presented similar docked poses where the alkyl chains were also buried inside the hydrophobic MD-2 pocket and the carboxylate moieties were establishing polar interactions with the resides at the MD-2 rim. Compounds **8** and **9** presented docked poses protruding slightly more than compound **7**, probably due to the longer alkyl chains, although the difference was very subtle (Figure S3, Supp. Info.).

To ensure the stability of the docked poses of compound **3** with TLR4/MD-2 and to gain insights on the interactions that take place, we performed 90 ns molecular dynamic simulations of the

(h)TLR4/MD-2/**3** complex starting from the docked geometries for both the antagonist and the agonist conformations of (h)TLR4/MD-2. In the simulation starting from the agonist conformation of MD-2 we could observe that compound **3** rotates of almost 90 degrees around its plan of symmetry (a partial rotation happens at 5 ns of simulation and the full rotation at approximately 38 ns) to find a more stable bound conformation that was maintained stable for the rest of the simulation (Figure S4, Supp. Info.). This rotation forced the MD-2 pocket to adopt an antagonist-like conformation (characterized by, inter alia, great motion of residue Phe126). In this new binding mode, two guanidinium groups of compound **3** continued to interact through hydrogen bonds with the side chains of Glu92, and Ser120, a third guanidinium group formed a new hydrogen bond with the CO group of Pro88, and the fourth guanidinium group was involved in polar interactions with the solvent. Moreover, later in the simulation (starting at 42 ns), the loop made by residues 80 to 90, undergoes a considerable deformation (Figure S5, Supp. Info.). In contrast, in the simulation of the TLR4/MD-2/**3** complex starting from the antagonist conformation, the geometries of both compound **3** and MD-2 were stable during the 90 ns run (Figure S5, Supp. Info.), not experiencing important conformational changes. These results clearly indicated that the complex of calixarene **3** with MD-2 in agonist conformation is less stable than the complex with the antagonist one, therefore providing explanations for the antagonist activity later observed (see below). Taken together, our computational studies provided plausible binding poses for compounds **2**-**4** into CD14 and for compounds **1**-**9** into TLR4/MD-2, supporting a putative direct binding to these proteins.

Synthesis

The already known guanidinocalixarenes **1**[35] and **3**-**6**[36, 37] were synthesized according to the procedures we already reported in the literature. Derivative **2,** previously reported, [32] was prepared from tetra-*t*-butyl-25,26,27,28-tetrabutylamino-calix[4]arene[38] through condensation with bis-BOC-*N*-triflylguanidine to obtain the protected precursor[32] and subsequent removal of the Boc protecting groups by treatment with 1% HCl in dioxane in presence of triethylsilane as scavenger. The anionic ligands **8** and **9** were obtained from the corresponding tetraacid derivatives[39] by titration with

NaOH, while the tetracarboxylate **7,** bearing hexyl chains at the lower rim, was obtained from the tetraformyl-tetrahexyl-calix[4]arene precursor[40] by oxidation with $NaClO_2$ in the presence of sulfamic acid and subsequent titration with NaOH.

Inhibition of LPS-stimulated TLR4 signal in HEK-Blue™ cells.

Calixarenes **1**-**9** were first screened for their capacity to interfere with LPS-stimulated TLR4 activation and signaling on HEK-Blue™ cells. HEK-Blue™ cells are stably transfected with TLR4, MD-2, and CD14 genes. In addition, these cells stably express an optimized alkaline phosphatase gene engineered to be secreted (sAP), placed under the control of a promoter inducible by several transcription factors such as NF-κB and AP-1.[36] This reporter gene allows monitoring the activation of TLR4 signal pathway by endotoxin. All calixarenes were inactive in stimulating TLR4 signal when provided alone thus indicating the absence of agonist activity, in agreement with the molecular modelling studies. On the other hand, compounds **1**-**5** inhibited in a dose-dependent way the LPS-stimulated TLR4 signal (Figure 6), while calixarene **6** with oxygenated ethylene-glycol chains instead of hydrocarbon chains showed weak antagonistic activity.

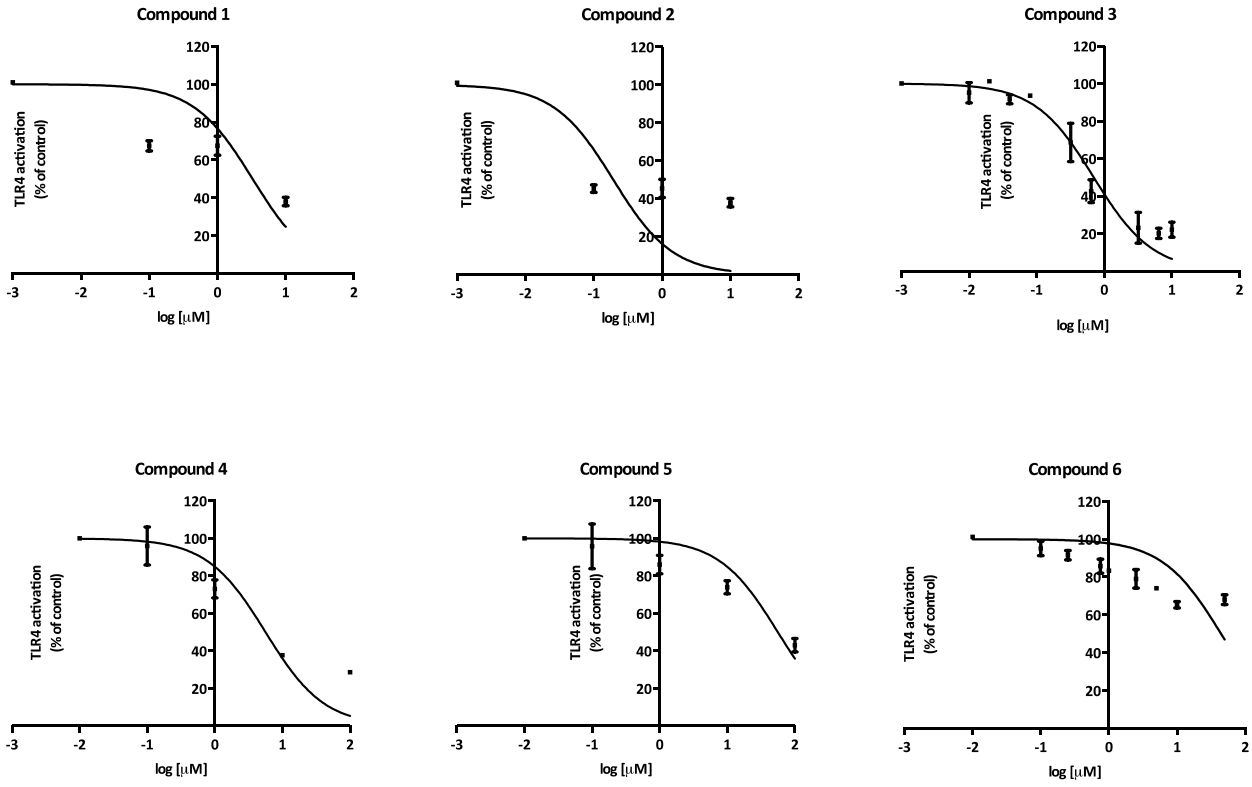

Figure 6. Dose dependent inhibition of LPS-stimulated HEK-Blue cells activation by calixarenes **1**-**5**. Human TLR4 HEK-Blue were treated with increasing concentrations of compounds and stimulated with LPS (100 ng/mL). The results represent normalized data with positive control (LPS alone) and expressed as the mean of percentage ± SD of at least three independent experiments.

Guanidinocalixarenes **1**-**5** inhibited TLR4 signal with potencies ranging from 0.2 to 63 µM (Table 1). Compounds **2**, **3** and **4** were the most potent antagonists and inhibited LPS-stimulated TLR4 signal with IC_{50} 0.2, 0.7 and 5.7 µM, respectively. In contrast, negatively charged amphiphilic calixarenes **7**-**9** with carboxylic acids on the upper rim showed no or very weak inhibition of LPS-TLR4 signal (Figure S9, Supp. Info.).

Compounds	IC_{50} LPS (µM)
1	10
2	0.2
3	0.7
4	5.7
5	63
6	45

Table 1. IC_{50} values for the inhibition of LPS-stimulated TLR4 signal in HEK cells

Inhibition of PHA lectin-stimulated TLR4 signal in HEK-Blue™ cells.

We were then interested in knowing if the inhibition of TLR4 signal is due to calixarene interaction with LPS or rather to a direct interaction with the TLR4 receptor system, evidenced as possible by calculations. To investigate this point, we stimulated HEK cells with the plant lectin phytohemagglutinin (PHA from *Phaseolus vulgaris*) whose property to potently stimulate TLR4 signal acting as agonist has been recently described.[41] We first checked if PHA is able to activate TLR4 signal in HEK-Blue cells, and we found that the lectin was active in stimulating in a dose-dependent way TLR4-dependent SEAP production (Figure S7, Supp. Info). To exclude the TLR4

activity could derive from LPS contamination in the PHA, we performed the experiment in the presence of the LPS-neutralizing peptide polymixin-B. We also verified that control HEK-null cells, that is HEK cells transfected with SEAP plasmid and lacking TLR4, MD-2, CD14 genes, were not activated by PHA lectin (Figure S7, Supp. Info). PHA lectin was then used instead of LPS as a TLR4 agonist to stimulate cells. The highly potent calixarene-based TLR4 antagonists, compounds **3** and **4**, were then investigated for their property to inhibit TLR4 activation by PHA lectin (Figure 7).

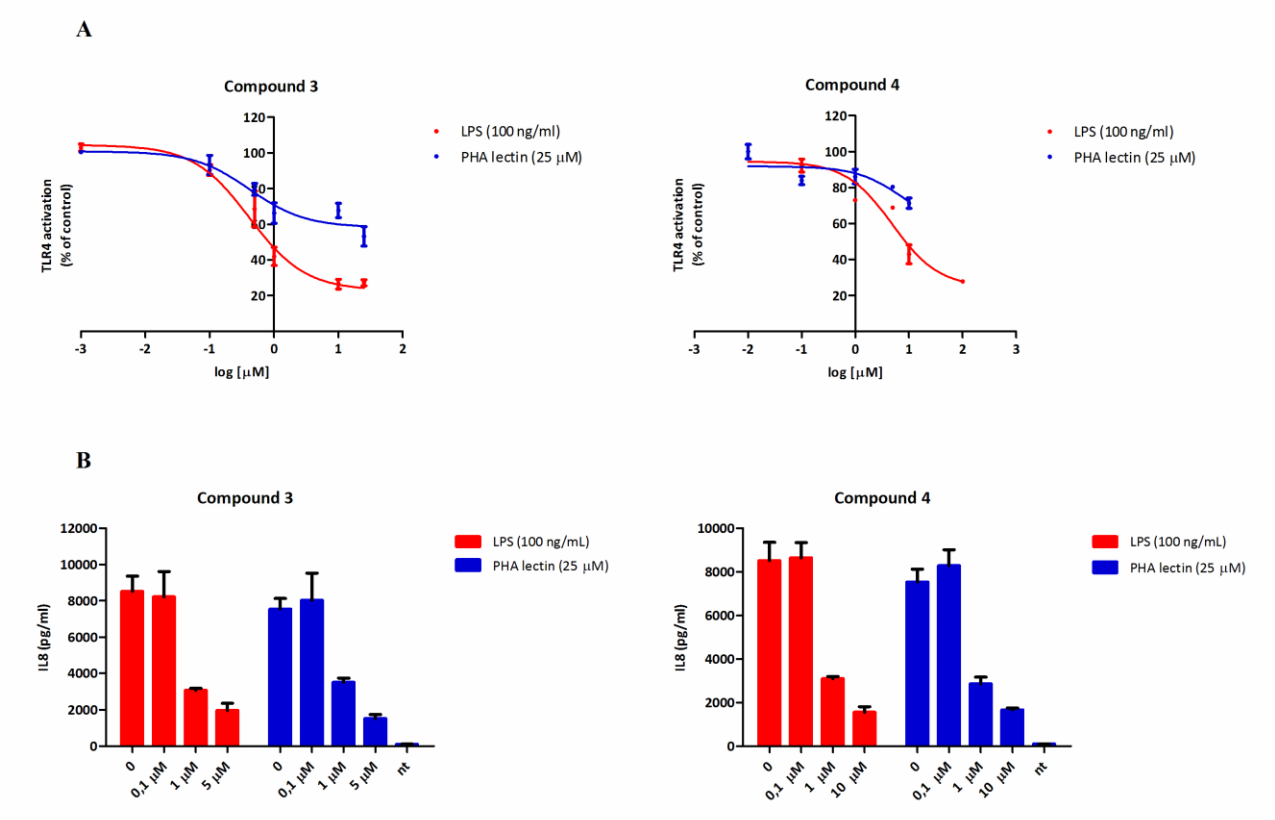

Figure 7. A) Inhibition of TLR4 signaling in HEK-Blue cells stimulated with LPS (100 ng/ml) or PHA lectin (25 µM) and treated with calixarenes **3** and **4**. The results represent normalized data with positive control (LPS or PHA lectin alone). B) Quantification of Interleukin-8 (IL-8) in HEK-Blue cells stimulated with LPS or PHA and treated with compounds **3** and **4** by performing ELISA assay. Data represent the mean of percentage ± SD of at least three independent experiments

Guanidinocalixarenes **3** and **4** were indeed active in inhibiting PHA lectin-stimulated TLR4 signal in a concentration-dependent way, with potencies similar to those measured in the inhibition of

LPS-stimulated TLR4 signal (Table 1). The fact that the antagonist activity was retained by calixarenes also when TLR4 was stimulated by a non-LPS agonist strongly suggests that the action of calixarenes is mainly based on direct interaction with CD14 and MD-2 receptors.

Inhibition of LPS-stimulated TLR4 signal in human white blood cells

As HEK cells are a non-natural system to study TLR4 activation and to perform preliminary screening, the capacity of lead compounds **3** and **4** to inhibit LPS-stimulated TLR4 signaling was further investigated in human white blood cells (h)WBCs that naturally express CD14, MD-2 and TLR4 receptors. We evaluated the production of the main NF-κB-dependent pro-inflammatory cytokines tumor necrosis factor alpha (TNFα), interleukin-6 (IL-6) and IL-8 by primary human Peripheral Blood Mononuclear Cells (hPBMCs) as readout for TLR4 pathway activation. hPBMCs isolated from the whole blood of healthy volunteers were treated with increasing concentrations (1-10 μM) of compounds **3** and **4** and stimulated after 30 min with LPS (100 ng/mL). Compounds **3** reduced the production of all the pro-inflammatory cytokines monitored, while compounds **4** showed a lower inhibitory activity, reducing only two of the three cytokines evaluated (Figure 8).

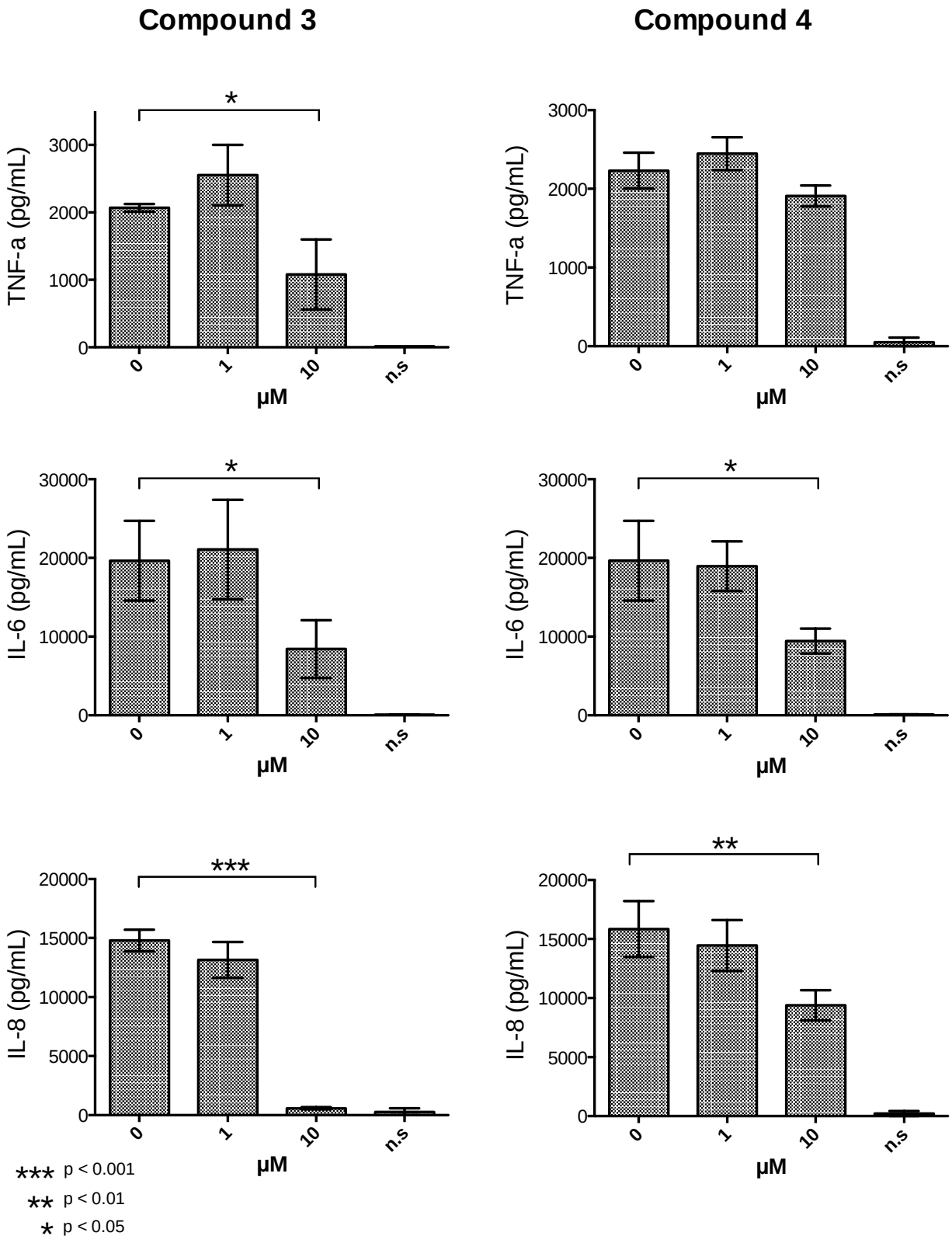

Figure 8. Inhibitory effect of compounds **3** and **4** on LPS-induced pro-inflammatory cytokines production by PBMCs. PBMCs isolated from whole blood were pre-incubated with synthetic compounds for 30 min and then stimulated with LPS (100 ng/mL). TNFα, IL-6 and IL-8 production

was quantified after one night's incubation. Data represent the mean ± SEM of at least three independent experiments.

Inhibition of LPS-stimulated TLR4 signal in murine White Blood Cells (m)WBCs

It is known that human and murine MD-2 have dissimilarities in the LPS binding region, and some ligands have different activity on (h)MD-2 and (m)MD-2, in some cases switching from agonism to antagonism. We therefore aimed to compare the activity of calixarene on human and murine cells. The activity of compounds **3** and **4** was then evaluated in a murine macrophages cell line, RAW-Blue™ cells. As HEK-Blue™ cells, RAW-Blue™ cells are transfected to stably express the SEAP reporter gene in order to monitor the activation of TLR4 signal pathway. Compounds **3** and **4** inhibited in a dose-dependent way the LPS-stimulated TLR4 signal (Figure 9A), revealing that the two calixarenes were also effective on the murine TLR4 system.

The abilities of compounds **3** and **4** were further investigated in murine splenocytes. TNF-α relative expression was determined from TLR4–MyD88 pathway activation. Splenocytes from balb/c mice were treated with two concentrations (1 and 10 µM) of compounds **3** and **4** in RPMI and stimulated after 30 min with LPS (100 ng/mL). The LPS-induced TNF-α expression after 5 hours incubation was measured by qPCR. The lower concentration of compounds **3** and **4** (1 µM) was weakly active in reducing LPS-induced TNF-α expression, whereas the higher concentration (10 µM) of both compounds completely inhibited the expression of TNF-α (Figure 9 B).

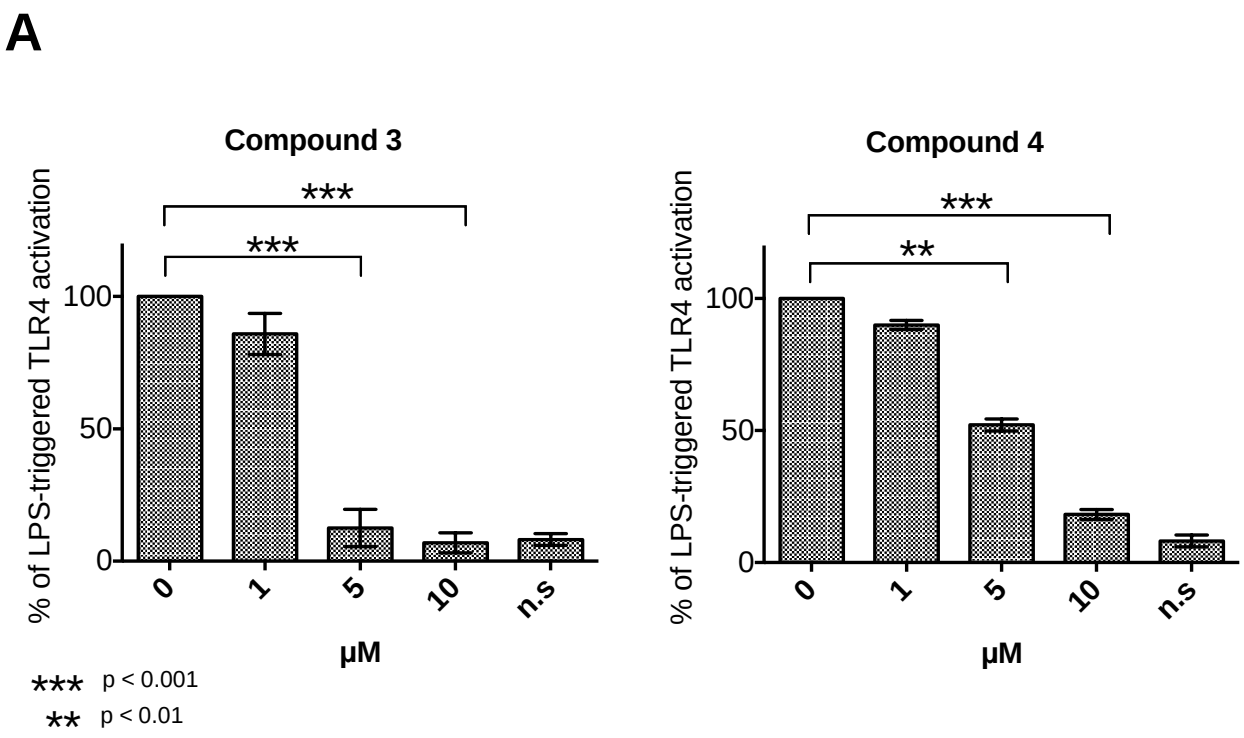

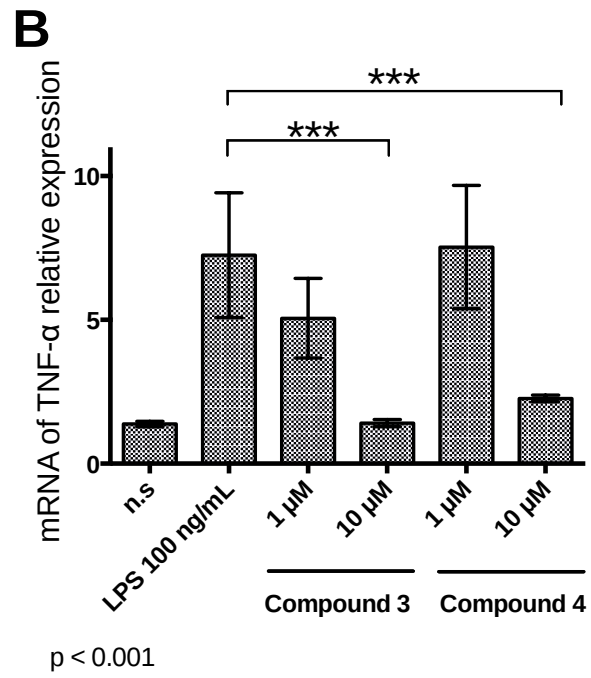

Figure 9. Effects of compounds **3** and **4** on Raw-Blue cells and on murine splenocytes. (A) RAW-Blue^{TM} cells stably transfected with NF-*k*B-dependent SEAP reporter plasmid were treated with increasing concentrations of compounds **3** and **4** and stimulated with LPS (100 ng/mL) after 30 min. Data represent the mean of percentage of at least three independent experiments.

(B) Murine splenocytes isolated from murine spleen were preincubated with two concentrations (1 and 10 μM) of compounds **3** and **4** for 30 min and then stimulated with LPS (100 ng/mL). Readout was the TNF-α expression after 5 hours of incubation. Normalized data are representative of three independent experiments.

Discussion and Conclusions

Calixarenes with guanidinium groups on one rim and hydrocarbon chains on the other are facial amphiphiles in which the charged polar face and the hydrophobic apolar one are spatially organized. Thanks to this structural feature, they can be potential modulators of the TLR4 activation through direct binding to the receptor or one of the co-receptors involved in the signaling process. We designed the series of calixarenes **1**-**9** aiming to explore the plausible direct binding to CD14 and MD-2 co-receptors. Docking studies demonstrated that compounds **2**-**4** and **1**-**9** are in principle able to form complexes with CD14 and TLR4.MD2 heterodimer (human and murine), respectively, independently from the relative disposition of the polar and apolar residues and from the nature of the charged groups. The lipophilic chains, linked at the upper (**1** and **2**) or at the lower (**3**-**5**) rim, resulted in all cases buried into the CD14 or MD-2 hydrophobic pocket, while the charged heads established contacts with polar residues located in proximity of the entry of the pockets. Therefore, our computational studies provide plausible binding poses into the TLR4 co-receptors for the investigated compounds and this supports our hypothesis of a direct binding of calixarene derivatives to these proteins in competition with LPS. These findings thus open the possibility to explore calixarenes as a platform for the design of TLR4/MD-2 modulators. Calculations on the stability of the complexes between the guanidinocalixarene **3** and TLR4/MD-2 suggested that this derivative, and for analogy at least all the other positively charged analogues, could act as antagonist.

The activity of positively charged calixarenes was tested on HEK cells expressing (h)TLR4/MD-2 and human and murine leukocytes. Cationic calixarenes **1**-**4** inhibited in a dose-dependent way LPS-stimulated TLR4 activation in both human and murine cells. Cells were first stimulated by

LPS and then treated with synthetic molecules. In agreement with the theoretical studies, compounds **1**-**4** showed an antagonist activity in the low micromolar range on human and murine TLR4. Paradoxically, negatively charged amphiphilic calixarenes, that should mimic better the anionic nature of lipid A, the natural MD-2 and CD14 ligand, were not active both in inhibiting and stimulating TLR4 Compound **6**, with more polar ether chains on the lower rim instead of hydrocarbon chains turned out to be substantially inactive as TLR4 inhibitor in both cell types. Additionally, calculations of the logP values predicted high values for compounds **7**, **8** and **9** (calculated logP values above 15), pointing to a high lipophilicity, while compound **6** was predicted to be extremely hydrophilic (calculated logP value below zero, Figure S6, Supp. Info.). These unfavourable values for logP could be correlated with poor physical-chemical properties thus explaining the lack of activity in the cells assays.

The very close IC_{50} values (Table 1) found for guanidinocalixarenes **2** and **3** evidence that the relative disposition of polar and hydrophobic residues with respect to the macrocyclic cavity does not have a significant impact on the inhibition activity of these ligands. Furthermore, by comparing compounds **3**-**5** it seems that an increasing lipophilicity results detrimental for the inhibition potency, even if the less amphiphilic derivative **6** is very poorly active with an IC_{50} two order of magnitude higher than that of **3**. A subtle balance between lipophilic and hydrophilic portions in the ligand structure seems then to be the key to determine the activity.

It is worth noting that lead compounds **3** and **4** show antagonist activity on both human and murine TLR4. Several TLR4 modulators resembling lipid A, have species-specific activity that is generally attributed, among other factors, to the dissimilarities in the shape of the hydrophobic binding pocket of (h) and (m)MD-2[42] and to the variations in the electrostatic potentials at the rim of the binding cavity of MD-2 and at the dimerization interface. The most significant example of this is the natural compound tetraacylated lipid IVa that acts as an antagonist on human but as an agonist on murine TLR4.[42] However, several synthetic phospho-glycolipids with a monosaccharide scaffold also showed agonist activity on murine and antagonist activity on human TLR4.[43]

Trying to understand whether the antagonist activity of calixarenes was due to their interaction with receptors or with LPSs, we also undertook studies of the TLR4 activation with non-LPS ligands. We reasoned that if the contribution of calixarenes in inhibiting TLR4 activation is due to a neutralizing effect on endotoxin, the antagonist effect would be lost by stimulating cells with a TLR4 agonist structurally different from LPS. Besides the natural agonists LPS, lipid A, lipid A mimetics as monophosphoryl lipid A (MPL),[44] and aminoalkyl glucosaminide 4-phosphates[19] (AGPs), TLR4 can also be activated by small molecules, such as the natural compound taxol,[45] oxidized phospholipids and synthetic pyrimido-indoles and neoseptins,[46, 47] and by protein DAMPs such as High Mobility Group Box1 (HMGB1)[48] and lectins. Lectins constitute a very large class of carbohydrate-binding proteins, and plant lectins have immunostimulating activity, that recently has been related to TLR agonism. In fact, the activity as potent TLR4 agonists of plant lectins KML-C (Korean mistletoe lectin)[49] and PHA (phytohaemagglutinin from *Phaseolus vulgaris*)[41] has been described. Although the experimental data indicate a strong TLR4 agonist activity by lectins, the mechanism of action of these proteins should still be clarified. Because lectins recognize and bind sugars, it is possible that lectins promote the formation of the $(TLR4/MD\text{-}2{\cdot}LPS)_2$ heterodimer by binding to the sugars attached to the surface of glycosylated MD-2 and TLR4 proteins thus bringing together two TLR4/MD-2 complexes.

According to these literature data, we first validated plant PHA lectin as agonist in HEK-Blue cells. A dose-dependent activation of TLR4 signal was observed when cells were treated with PHA lectin in the presence of polymixin-B to neutralize the agonist effect of any possible LPS contamination. The addition of calixarenes **1**-**4** followed by lectins inhibited in a dose-dependent way the TLR4 signal, showing that cationic calixarenes antagonize TLR4 signal also in the case of non-LPS stimulation. This would suggest a direct interaction of calixarenes with CD14 and MD-2 receptors, according to the predicted binding poses by docking calculations and molecular dynamic simulations. Calixarenes **3** and **4** showed a potent TLR4 antagonist activity in cells and inhibited the production of the inflammatory TNF-α production in LPS-stimulated murine splenocytes and in mice. Although

solubility and distribution properties of calixarenes **3** and **4** should be optimized for in vivo studies and preclinical development, the lack of toxicity (Figure S8, Supp. Info.) and the potent TLR4 blocking activity point to these compounds as plausible drug hits targeting TLR4. The flexibility of calixarene scaffold will allow to modulate the hydrophilicity profile of cationic amphiphiles and optimize their pharmacokinetic. The possibility of the calix cavity to complex metal ions or small organic fluorophores could also be exploited to generate labeled compounds for diagnostic and therapeutic applications.

Experimental section

Molecular modeling

Structure construction. 3D structures of the ligands were built with PyMOL molecular graphics and modelling package[50] based on the coordinates of the calixarene scaffold retrieved from the PubChem database (CID:562409). 3D Coordinates for the agonist hTLR4/MD-2 complex, the antagonist mTLR4/MD-2 complex, the agonist mTLR4/MD-2 complex and hCD14 were retrieved from the PDB database (www.rcsb.org), under the ID 3FXI, 2Z64, 3VQ2 and 4GLP, respectively. The structures went through a restrained minimization procedure with Maestro using the OPLS3 force field. Gasteiger charges were computed within the AutoDock Tools program and all non-polar hydrogens were merged.

Structure optimization. All compounds (from **1** to **9**) were optimized with *ab initio* calculations, using the density functional theory (DFT) with the hybrid functional B3LYP with the Pople basis set 6-31+g(d,p) using Gaussian g09/e1[51]. Water solvation (with a dielectric constant of ε=78.3553) was simulated with the Gaussian default SCRF method (i.e. using the Polarizable Continuum Model (PCM) with the integral equation formalism variant (IEFPCM)).

Docking procedure. Docking was performed independently with both AutoDock 4.2[52] and AutoDock VINA 1.1.2[53]. In AutoDock 4.2, the Lamarckian evolutionary algorithm was chosen and all parameters were kept default except for the number of genetic algorithm (GA) runs which was set to 200 to enhance the sampling. AutoDockTools 1.5.6 was used to assign the Gasteiger-Marsili

empirical atomic partial charges to the atoms of both the ligands and the receptors. The structure of the receptors was always kept rigid whereas the structure of the ligand was set partially flexible by providing freedom to some appropriately selected dihedral angles.

Concerning the boxes, spacing was set to 0.375 Å for AutoDock and is default to 1Å for VINA. In the case of the human and mouse TLR4/MD-2 systems in their agonist and antagonist conformations, the size of the box was set to 33.00 Å in the x-axis, 40.50Å in the y-axis and 35.25 Å in the z-axis. For (h)CD14 the size of the box was set to 33.00 Å in the x-axis, 33.75Å in the y-axis and 33.75 Å in the z-axis. For the (h)TLR4/MD-2 complex the center of the box is located equidistant to the center of mass of residues Arg90 (MD-2), Lys122 (MD-2) and Arg264 (TLR4). For the (m)TLR4/MD-2 complex the center of the box is located equidistant to the center of mass of residues Arg90 (MD-2), Glu122 (MD-2) and Lys263 (TLR4). For (h)CD14 the center of the box is located equidistant to the center of mass of residues Phe69, Tyr82 and Leu89.

Parameters derivation. Parameters for molecular dynamics simulations were set up with the standard Antechamber[54] procedure. Briefly, charged were calculated with Gaussian at the Hartree-Fock level (HF/6-31G* Pop=MK iop(6/33=2) iop(6/42=6)) from the solvated DFT B3LYP optimized structure, then derived and formatted for Ambertools15 and Amber14[55] with Antechamber assigning the general AMBER force field (GAFF) atom types [56]. A new atom type for nitrogen was introduced (nj), within GAFF, to properly describe the guanidine moiety, mirroring the parameters of ff14SB[57] used to describe the guanidine fragment present in arginine. Parameters for this new atom are provided in the supplementary information section.

Molecular Dynamics (MD) simulations. Before being submitted to the production run, the system undergoes a height steps preparation. The first one consists of 1000 steps of steepest descent algorithm followed by 7000 steps of conjugate gradient algorithm; a 100 $kcal.mol^{-1}.A^{-2}$ harmonic potential constraint is applied on both the proteins and the ligand. In the 4 subsequent steps, the harmonic potential is progressively lowered (respectively to 10, 5 and 2.5 $kcal.mol^{-1}.A^{-}$) for 600 steps of conjugate gradient algorithm each time, and then the whole system is minimized uniformly. In the

following step the system is heated from 0 K to 100 K using the Langevin thermostat in the canonical ensemble (NVT) while applying a 20 $kcal.mol^{-1}.A^{-2}$ harmonic potential restraint on the proteins and the ligand. The next step heats up the system from 100 K to 300 K in the Isothermal–isobaric ensemble (NPT) under the same restraint condition than the previous step. In the last step the same parameters are used to simulate the system for 100 ps but no harmonic restraint is applied. At this point the system is ready for the production run, which is performed using the Langevin thermostat under NPT ensemble, at a 2 fs time step. All production runs were performed for 90 ns.

LogP calculations. From the optimized 3D structure of compounds **1**-**9**, logP value was calculated with Maestro package (www.schrodinger.com/maestro).

Biology: cell tests

HEK-Blue activation assay

HEK-Blue-TLR4 cells (InvivoGen) were cultured according to manufacturer's instructions. Briefly, cells were cultured in DMEM high glucose medium supplemented with 10% fetal bovine serum (FBS), 2 mM glutamine, 1x Penstrep, 1× Normocin (InvivoGen), 1× HEK-Blue Selection (InvivoGen). Cells were detached by trypsin and the cell concentration was estimated by using Trypan Blue (Sigma-Aldrich). The cells were diluted in DMEM high glucose medium supplemented as described before and seeded in multiwell plate at a density of 2×10^4 cells per well in 200 µL. After overnight incubation (37 °C, 5% CO_2, 95% humidity), supernatant was removed, cell monolayers were washed with warm PBS and treated with increasing concentrations of compounds dissolved in water or DMSO−ethanol (1:1) and diluted in DMEM. After 30 min, the cells were stimulated with 100 ng/mL LPS from *E. coli* O55:B5 (Sigma- Aldrich) or 25 µM lectin from *Phaseolus vulgaris* (PHA-P) and incubated overnight. As control, the cells were treated with or without LPS (100 ng/mL) or PHA-P (25 µM) alone. Then the supernatants were collected and 50 µL of each sample were added to 100 µL PBS, pH 8, 0.84 mM paranitrophenylphosphate (pNPP) for a final concentration of 0.8 mM pNPP. Plates were incubated for 2−4 h in the dark at room temperature, and then the plate reading was assessed by using a spectrophotometer at 405 nm (LT 4000, Labtech).

The results were normalized with positive control (LPS or PHA-P alone) and expressed as the mean of percentage ± SD of at least three independent experiments. As control, the same procedure was performed in HEK-Blue Null cells, the parental cell line of TLR4 Hek Blue.

Human Peripheral Blood Mononuclear cells (hPBMCs).

Whole blood was collected from healthy volunteers. Informed consent was obtained from all volunteers. Research using biological samples from mice was performed in accordance with institutional guidelines defined by EU Directive 2010/63/EU for Europe.

Whole blood was diluted 1:1 with PBS, and layered on Lymphoprep® (STEMCELL Technologies) for density gradient centrifugation according to the manufacturer's instructions. PBMCs were harvested from the interface, washed in PBS and resuspended in complete RPMI with 10% FBS, 2 mM glutamine and antibiotics. Informed consent was obtained from all volunteers. Cells were then plated in a 96 multi-well plate (10^5 cells/well) in presence of different concentrations of the two compounds to be tested. After 30' cells were stimulated with 100 ng/mL of LPS and incubated for 18 hours (37°C, 5% CO_2, 95% humidity). Cells supernatants were harvested and TNF-α, IL-6 and IL-8 cytokines were quantified by ELISA assay (R&D Systems; #DY206-05, # DY210-05, # DY208-05) according to manufacturer's instructions. The optical density of wells were determined using a microplate reader set to 450 nm (LT 4000, Labtech). All graphs were representative data from at least three independent experiments.

RAW-Blue cells

Raw-Blue cells (InvivoGen) were cultured according to manufacturer's instructions. Briefly, cells were cultured in DMEM high glucose medium supplemented with 10% fetal bovine serum (FBS), 2 mM glutamine, 100 µg/mL Normocin (InvivoGen), 200 µg/mL Zeocin (InvivoGen). Cells were detached using a cell scraper and the cell concentration was estimated by using Trypan Blue (Sigma-Aldrich). The cells were diluted in DMEM high glucose medium supplemented as described before and seeded in multi-well plate at a density of 6×10^4 cells cells per well in 200 µL. After overnight incubation (37 °C, 5% CO_2, 95% humidity), supernatant was removed, cell monolayers were washed

with warm PBS and treated with increasing concentrations of compounds dissolved in DMSO−ethanol (1:1) and diluted in DMEM. After 30 min, the cells were stimulated with 100 ng/mL LPS from *E. coli* O55:B5 (Sigma- Aldrich). Then the supernatants were collected and 50 µL of each sample were added to 100 µL PBS, pH 8, 0.84 mM paranitrophenylphosphate (pNPP) for a final concentration of 0.8 mM pNPP. Plates were incubated for 2−4 h in the dark at room temperature, and then the plate reading was assessed by using a spectrophotometer at 405 nm (LT 4000, Labtech). The results were normalized with positive control (LPS alone) and expressed as the mean of percentage ± SD of at least three independent experiments.

Murine splenocytes.

Murine splenocytes were isolated from the spleen of balb/c mice (11−13 weeks old), counted and resuspended in complete RPMI with 10% FBS, 2 mM glutamine and antibiotics. Cells were then plated in a 24 multi-well plate ($1{,}5x10^6$ cells/well) in presence of different concentrations of the two compounds to be tested. After 30' cells were stimulated with 100 ng/mL of LPS and incubated for 5 hours (37°C, 5% CO_2, 95% humidity). Cells were lysed and total RNA was isolated by means of the Quick-RNA™MiniPrep purification kit (Zymo Research; R1054). TNF-α expression analyses were performed by real-time qPCR. Gene induction fold changes were normalized to β-actin, shown as mean and SEM of two technical replicates. All graphs were representative data from at least three independent experiments.

MTT Cell Viability Assay.

Human embryonic kidney (HEK) 293 cells were grown in DMEM supplemented with 10% FBS, 2mM glutamine and Penstrep 1x. The cells were seeded in 100 µL of DMEM without Phenol Red at a density of 2×10^4 cells per well 100 µL and incubated overnight (37 °C, 5% CO_2, 95% humidity). Then, the cells were treated with 10 µL of compounds, dissolved in DMSO- ethanol and diluted in DMEM, and incubated again. DMSO 5% and PBS were included as controls. The day after, 10 µL of MTT solution (5 mg/mL in PBS) were added to each well and after 3 h incubation, HCl 0.1 N in 2-propanol was added (100 µL per well) to dissolve formazan crystals. Formazan concentration in

the wells was determined by measuring the absorbance at 570 nm (LT 4000, Labtech). The results were normalized with untreated control (PBS) and expressed as the mean of percentage ± SD of three independent experiments.

IL-8 quantification

Supernatants from HEK- Blue cells treated with compounds **3** (0.1, 1, 5 μM) and **4** (0.1, 1, 10 μM) and stimulated with LPS (100 ng/mL) or PHA-P (25 μM) were used to quantify IL-8 concentration by performing ELISA assay (Thermo scientific) according to manufacturer's instructions. The readings were assessed by using a spectrophotometer at 450 nm (LT 4000, Labtech).

PAINS

Compounds **1-9** were subjected to the pan assay interference compounds (PAINS) on-line filter (ZINC PAINS patterns search http://zinc15.docking.org/patterns/home/, accessed Jan 26, 2016) and substructure filters.[58] This analysis showed that none of them were PAINS.

Acknowledgements

This study was financially supported by the H2020-MSC-ETN-642157 project TOLLerant. The Italian Ministry for Foreign Affairs and International Cooperation (MAECI), the Italian Ministry of Instruction, University and Research (MIUR, PRIN2010JMAZML MultiNanoIta), the COST Action CM1102 'MultiGlycoNano', and the Spanish Ministry for Economy and Competitiveness (MINECO) grant CTQ2014-57141-R are also acknowledged.

Corresponding Authors:

Francesco Peri, Phone: +39.02.64483453; E-mail: francesco.peri@unimib.it;

Francesco Sansone, Phone: +39.0521.905458; E-mail: francesco.sansone@unipr.it.

Abbreviations: TLR, Toll-like receptor; PRRs, pattern recognition receptors; PAMPs, pathogen-associated molecular patterns; MD-2, myeloid differentiation 2; PHA, phytohaemagglutinin; LOS,

lipooligosaccharide; DC, dendritic cells; DAMPs, damage-associated molecular patterns; RA, rheumathoid arthritis; ALS, amyotrophic lateral sclerosis; LBP, lipid binding protein; CD14, cluster of differentiation 14; AMP, antimicrobial peptides; hPBMC, human peripheral blood mononuclear cells; IL, interleukin.

Supporting Information: Molecular Modeling, Docking Results; Chemistry: Synthesis and compounds characterization, molecular formula strings; Biology: activity of PHA plant lectin and of compounds **7**-**9** on HEK cells, MTT toxicity test.

References

1. Akira, S.; Takeda, K. Toll-like Receptor Signalling. *Nat. Rev. Immunol.* **2004,** *4*, 499-511.

2. Poltorak, A.; He, X.; Smirnova, I.; Liu, M.; Van Huffel, C.; Du, X.; Birdwell, D.; Alejos, E.; Silva, M.; Galanos, C.; Freudenberg, M.; Ricciardi-Castagnoli, P.; Layton, B.; Beutler, B. Defective LPS Signaling in C3H/HeJ and C57BL/10ScCr Mice: Mutations in Tlr4 Gene. *Science.* **1998,** *282*, 2085-2088.

3. Gioannini, T.; Teghanemt, A.; Zhang, D.; Coussens, N.; Dockstader, W.; Ramaswamy, S.; Weiss, J. Isolation of an Endotoxin-MD-2 Complex that Produces Toll-like Receptor 4-dependent Cell Activation at Picomolar Concentrations. *Proc. Natl. Acad. Sci. U. S. A.* **2004,** *101*, 4186-4191.

4. Park, B.; Song, D.; Kim, H.; Choi, B.; Lee, H.; Lee, J. The Structural Basis of Lipopolysaccharide Recognition by the TLR4-MD-2 Complex. *Nature.* **2009,** *458*, 1191-1195.

5. Gogos, C. A.; Drosou, E.; Bassaris, H. P.; Skoutelis, A. Pro- versus Anti-inflammatory Cytokine Profile in Patients with Severe Sepsis: a Marker for Prognosis and Future Therapeutic Options. *J. Infect. Dis.* **2000,** *181*, 176-180.

6. Brunialti, M.; Martins, P.; Barbosa de Carvalho, H.; Machado, F.; Barbosa, L.; Salomao, R. TLR2, TLR4, CD14, CD11B, and CD11C Expressions on Monocytes Surface and Cytokine Production in Patients with Sepsis, Severe Sepsis, and Septic Shock. *Shock.* **2006,** *25*, 351-357.

7. Erridge, C. The Roles of Toll-like Receptors in Atherosclerosis. *J. Innate. Immun.* **2009,** *1*, 340-349.

8. Abdollahi-Roodsaz, S.; Joosten, L. A.; Roelofs, M. F.; Radstake, T. R.; Matera, G.; Popa, C.; van der Meer, J. W.; Netea, M. G.; van den Berg, W. B. Inhibition of Toll-like Receptor 4 Breaks The Inflammatory Loop in Autoimmune Destructive Arthritis. *Arthritis Rheum.* **2007,** *56*, 2957-2967.

9. Cao, L.; Tanga, F. Y.; Deleo, J. A. The Contributing Role of CD14 in Toll-like Receptor 4 Dependent Neuropathic Pain. *Neuroscience.* **2009,** *158*, 896-903.

10. Casula, M.; Iyer, A. M.; Spliet, W. G.; Anink, J. J.; Steentjes, K.; Sta, M.; Troost, D.; Aronica, E. Toll-like Receptor Signaling in Amyotrophic Lateral Sclerosis Spinal Cord Tissue. *Neuroscience.* **2011,** *179*, 233-243.

11. Andreu, D.; Rivas, L. Animal Antimicrobial Peptides: an Overview. *Biopolymers.* **1998,** *47*, 415-433.

12. Rifkind, D. Studies on the Interaction Between Endotoxin and Polymyxin B. *J. Infect. Dis.* **1967,** *117*, 433-438.

13. David, S. Towards a Rational Development of Anti-endotoxin Agents: Novel Approaches to Sequestration of Bacterial Endotoxins with Small Molecules. *J. Mol. Recognit.* **2001,** *14*, 370-387.

14. Burns, M.; Jenkins, S.; Kimbrell, M.; Balakrishna, R.; Nguyen, T.; Abbo, B.; David, S. Polycationic Sulfonamides for the Sequestration of Endotoxin. *J. Med. Chem.* **2007,** *50*, 877-888.

15. Ohto, U.; Fukase, K.; Miyake, K.; Satow, Y. Crystal Structures of Human MD-2 and its Complex with Antiendotoxic Lipid IVa. *Science.* **2007,** *316*, 1632-1634.

16. Takayama, K.; Qureshi, N.; Beutler, B.; Kirkland, T. N. Diphosphoryl Lipid A from Rhodopseudomonas sphaeroides ATCC 17023 Blocks Induction of Cachectin in Macrophages by Lipopolysaccharide. *Infect. Immun.* **1989,** *57*, 1336-1338.

17. Mullarkey, M.; Rose, J.; Bristol, J.; Kawata, T.; Kimura, A.; Kobayashi, S.; Przetak, M.; Chow, J.; Gusovsky, F.; Christ, W.; Rossignol, D. Inhibition of Endotoxin Response by e5564, a Novel Toll-like Receptor 4-directed Endotoxin Antagonist. *J. Pharmacol. Exp. Ther.* **2003,** *304*, 1093-1102.

18. Rossignol, D.; Lynn, M. Antagonism of in vivo and ex vivo Response to Endotoxin by E5564, a Synthetic Lipid A Analogue. *J. Endotoxin Res.* **2002,** *8*, 483-488.

19. Johnson, D.; Sowell, C.; Johnson, C.; Livesay, M.; Keegan, D.; Rhodes, M.; Ulrich, J.; Ward, J.; Cantrell, J.; Brookshire, V. Synthesis and Biological Evaluation of a New Class of Vaccine Adjuvants: Aminoalkyl Glucosaminide 4-phosphates (AGPs). *Bioorg. Med. Chem. Lett.* **1999,** *9*, 2273-2278.

20. Lewicky, J. D.; Ulanova, M.; Jiang, Z. H. Improving the Immunostimulatory Potency of Diethanolamine-containing Lipid A Mimics. *Bioorg. Med. Chem.* **2013,** *21*, 2199-2209.

21. Funatogawa, K.; Matsuura, M.; Nakano, M.; Kiso, M.; Hasegawa, A. Relationship of Structure and Biological Activity of Monosaccharide Lipid A Analogues to Induction of Nitric Oxide Production by Murine Macrophage RAW264.7 cells. *Infect. Immun.* **1998,** *66*, 5792-5798.

22. Kim, H. M.; Park, B. S.; Kim, J. I.; Kim, S. E.; Lee, J.; Oh, S. C.; Enkhbayar, P.; Matsushima, N.; Lee, H.; Yoo, O. J.; Lee, J. O. Crystal Structure of the TLR4-MD-2 Complex with Bound Endotoxin Antagonist Eritoran. *Cell.* **2007,** *130*, 906-917.

23. Shirey, K. A.; Lai, W.; Scott, A. J.; Lipsky, M.; Mistry, P.; Pletneva, L. M.; Karp, C. L.; McAlees, J.; Gioannini, T. L.; Weiss, J.; Chen, W. H.; Ernst, R. K.; Rossignol, D. P.; Gusovsky, F.; Blanco, J. C.; Vogel, S. N. The TLR4 Antagonist Eritoran Protects Mice from Lethal Influenza Infection. *Nature.* **2013**, *497*, 498-502.

24. Piazza, M.; Yu, L.; Teghanemt, A.; Gioannini, T.; Weiss, J.; Peri, F. Evidence of a Specific Interaction between New Synthetic Antisepsis Agents and CD14. *Biochemistry.* **2009,** *48*, 12337-12344.

25. De Paola, M.; Sestito, S. E.; Mariani, A.; Memo, C.; Fanelli, R.; Freschi, M.; Bendotti, C.; Calabrese, V.; Peri, F. Synthetic and Natural Small Molecule TLR4 Antagonists Inhibit Motoneuron Death in Cultures from ALS Mouse Model. *Pharmacol. Res.* **2016,** *103*, 180-187.

26. Shirey, K. A.; Lai, W.; Patel, M. C.; Pletneva, L. M.; Pang, C.; Kurt-Jones, E.; Lipsky, M.; Roger, T.; Calandra, T.; Tracey, K. J.; Al-Abed, Y.; Bowie, A. G.; Fasano, A.; Dinarello, C. A.; Gusovsky, F.; Blanco, J. C.; Vogel, S. N. Novel Strategies For Targeting Innate Immune Responses to Influenza. *Mucosal. Immunol.* **2016**, *9*, 1173-1182.

27. Rodriguez Lavado, J.; Sestito, S. E.; Cighetti, R.; Aguilar Moncayo, E. M.; Oblak, A.; Lainšček, D.; Jiménez Blanco, J. L.; García Fernández, J. M.; Ortiz Mellet, C.; Jerala, R.; Calabrese, V.; Peri, F. Trehalose- and Glucose-derived Glycoamphiphiles: Small-molecule and Nanoparticle Toll-like Receptor 4 (TLR4) Modulators. *J. Med. Chem.* **2014,** *57*, 9105-9123.

28. Giuliani, M.; Morbioli, I.; Sansone, F.; Casnati, A. Moulding Calixarenes for Biomacromolecule Targeting. *Chem. Commun.* **2015,** *51*, 14140-14159.

29. Salvio, R.; Volpi, S.; Cacciapaglia, R.; Casnati, A.; Mandolini, L.; Sansone, F. Ribonuclease Activity of an Artificial Catalyst That Combines a Ligated Cu(II) Ion and a Guanidinium Group at the Upper Rim of a cone-Calix[4]arene Platform. *J. Org. Chem.* **2015,** *80*, 5887-5893.

30. Avvakumova, S.; Fezzardi, P.; Pandolfi, L.; Colombo, M.; Sansone, F.; Casnati, A.; CProsperi, D. Gold Nanoparticles Decorated by Clustered Multivalent Cone-Glycocalixarenes Actively Improve the Targeting Efficiency Toward Cancer Cells. *Chem. Commun.* **2014,** *50*, 11029-11032.

31. Mochizuki, S.; Nishina, K.; Fujii, S.; Sakurai, K. The Transfection Efficiency of Calix[4]arene-based Lipids: The Role of the Alkyl Chain Length. *Biomater. Sci.* **2015,** *3*, 317-322.

32. Chen, X.; Dings, R. P.; Nesmelova, I.; Debbert, S.; Haseman, J. R.; Maxwell, J.; Hoye, T. R.; Mayo, K. H. Topomimetics of Amphipathic Beta-sheet and Helix-forming Bactericidal Peptides Neutralize Lipopolysaccharide Endotoxins. *J. Med. Chem.* **2006,** *49*, 7754-7765.

33. Cighetti, R.; Ciaramelli, C.; Sestito, S. E.; Zanoni, I.; Kubik, Ł.; Ardá-Freire, A.; Calabrese, V.; Granucci, F.; Jerala, R.; Martín-Santamaría, S.; Jiménez-Barbero, J.; Peri, F. Modulation of CD14 and TLR4·MD-2 Activities by a Synthetic Lipid A Mimetic. *Chembiochem.* **2014,** *15*, 250-258.

34. Ciaramelli, C.; Calabrese, V.; Sestito, S. E.; Pérez-Regidor, L.; Klett, J.; Oblak, A.; Jerala, R.; Piazza, M.; Martín-Santamaría, S.; Peri, F. Glycolipid-based TLR4 Modulators and Fluorescent Probes: Rational Design, Synthesis, and Biological Properties. *Chem. Biol. Drug. Des.* **2016,** *88*, 217-229.

35. Bagnacani, V.; Sansone, F.; Donofrio, G.; Baldini, L.; Casnati, A.; Ungaro, R. Macrocyclic Nonviral Vectors: High Cell Transfection Efficiency and Low Toxicity in a Lower Rim Guanidinium Calix[4]arene. *Org. Lett.* **2008,** *10*, 3953-3956.

36. Sansone, F.; Dudic, M.; Donofrio, G.; Rivetti, C.; Baldini, L.; Casnati, A.; Cellai, S.; Ungaro, R. DNA Condensation and Cell Transfection Properties of guanidinocalixarenes: Dependence on Macrocycle Lipophilicity, Size, and Conformation. *J. Am. Chem. Soc.* **2006,** *128*, 14528-14536.

37. Baldini, L.; Cacciapaglia, R.; Casnati, A.; Mandolini, L.; Salvio, R.; Sansone, F.; Ungaro, R. Upper Rim Guanidinocalix[4]arenes as Artificial Phosphodiesterases. *J. Org. Chem.* **2012,** *77*, 3381-3389.

38. Barboso, S.; Garcia Carrera, A.; Matthews, S. E.; Arnaud-Neu, F.; Böhmer, V.; Dozol, J.-F.; Rouquette, H.; Schwing-Weill, M.-J. Calix[4]arenes with CMPO Functions at the Narrow Rim. Synthesis and Extraction Properties. *J. Chem. Soc., Perkin Trans. 2* **1999**, 719-723.

39. Nomura, E.; Hosoda, A.; Takagaki, M.; Mori, H.; Miyake, Y.; Shibakami, M.; Taniguchi, H. Self-organized Honeycomb-patterned Microporous Polystyrene thin Films Fabricated by calix[4]arene Derivatives. *Langmuir.* **2010,** *26*, 10266-10270.

40. Gallego-Yerga, L.; Lomazzi, M.; Franceschi, V.; Sansone, F.; Ortiz Mellet, C.; Donofrio, G.; Casnati, A.; García Fernández, J. M. Cyclodextrin- and Calixarene-based Polycationic Amphiphiles as Gene Delivery Systems: a Structure-activity Relationship Study. *Org. Biomol. Chem.* **2015,** *13*, 1708-1723.

41. Unitt, J.; Hornigold, D. Plant Lectins are Novel Toll-like Receptor Agonists. *Biochem. Pharmacol.* **2011,** *81*, 1324-1328.

42. Ohto, U.; Fukase, K.; Miyake, K.; Shimizu, T. Structural Basis of Species-specific Endotoxin Sensing by Innate Immune Receptor TLR4/MD-2. *Proc. Natl. Acad. Sci. U. S. A.* **2012,** *109*, 7421-7426.

43. Matsuura, M.; Kiso, M.; Hasegawa, A. Activity of Monosaccharide Lipid A Analogues in Human Monocytic Cells as Agonists or Antagonists of Bacterial Lipopolysaccharide. *Infect. Immun.* **1999,** *67*, 6286-6292.

44. Ulrich, J.; Myers, K. Monophosphoryl Lipid A as an Adjuvant. Past Experiences and New Directions. *Pharm. Biotechnol.* **1995,** *6*, 495-524.

45. Resman, N.; Gradisar, H.; Vasl, J.; Keber, M.; Pristovsek, P.; Jerala, R. Taxanes Inhibit Human TLR4 Signaling by Binding to MD-2. *FEBS Lett.* **2008,** *582*, 3929-3934.

46. Morin, M. D.; Wang, Y.; Jones, B. T.; Su, L.; Surakattula, M. M.; Berger, M.; Huang, H.; Beutler, E. K.; Zhang, H.; Beutler, B.; Boger, D. L. Discovery and Structure-Activity Relationships of the Neoseptins: A New Class of Toll-like Receptor-4 (TLR4) Agonists. *J. Med. Chem.* **2016,** *59*, 4812-4830.

47. Wang, Y.; Su, L.; Morin, M. D.; Jones, B. T.; Whitby, L. R.; Surakattula, M. M.; Huang, H.; Shi, H.; Choi, J. H.; Wang, K. W.; Moresco, E. M.; Berger, M.; Zhan, X.; Zhang, H.; Boger, D. L.; Beutler, B. TLR4/MD-2 Activation by a Synthetic Agonist with no Similarity to LPS. *Proc. Natl. Acad. Sci. U. S. A.* **2016,** *113*, E 884-893.

48. Goligorsky, M. S. TLR4 and HMGB1: Partners in Crime? *Kidney Int.* **2011**, *80*, 450-452.

49. Park, H. J.; Hong, J. H.; Kwon, H. J.; Kim, Y.; Lee, K. H.; Kim, J. B.; Song, S. K. TLR4-mediated Activation of Mouse Macrophages by Korean Mistletoe Lectin-C (KML-C). *Biochem. Biophys. Res. Commun.* **2010,** *396*, 721-725.

50. Schrodinger, LLC. PyMOL Molecular Graphics System, Version 1.8. **2015**.

51. Frisch, M. J.; Trucks, G. W.; Schlegel, H. B.; Scuseria, G. E.; Robb, M. A.; Cheeseman, J. R.; Scalmani, G.; Barone, V.; Mennucci, B.; Petersson, G. A.; Nakatsuji, H.; Caricato, M.; Li, X.; Hratchian, H. P.; Izmaylov, A. F.; Bloino, J.; Zheng, G.; Sonnenberg, J. L.; Hada, M.; Ehara, M.; Toyota, K.; Fukuda, R.; Hasegawa, J.; Ishida, M.; Nakajima, T.; Honda, Y.; Kitao, O.; Nakai, H.; Vreven, T.; Montgomery Jr., J. A.; Peralta, J. E.; Ogliaro, F.; Bearpark, M. J.; Heyd, J.; Brothers, E. N.; Kudin, K. N.; Staroverov, V. N.; Kobayashi, R.; Normand, J.; Raghavachari, K.; Rendell, A. P.; Burant, J. C.; Iyengar, S. S.; Tomasi, J.; Cossi, M.; Rega, N.; Millam, N. J.; Klene, M.; Knox, J. E.; Cross, J. B.; Bakken, V.; Adamo, C.; Jaramillo, J.; Gomperts, R.; Stratmann, R. E.; Yazyev, O.;

Austin, A. J.; Cammi, R.; Pomelli, C.; Ochterski, J. W.; Martin, R. L.; Morokuma, K.; Zakrzewski, V. G.; Voth, G. A.; Salvador, P.; Dannenberg, J. J.; Dapprich, S.; Daniels, A. D.; Farkas, Ö.; Foresman, J. B.; Ortiz, J. V.; Cioslowski, J.; Fox, D. J. *Gaussian 09*, Gaussian, Inc.: Wallingford, CT, USA, **2009**.

52. Morris, G. M.; Huey, R.; Lindstrom, W.; Sanner, M. F.; Belew, R. K.; Goodsell, D. S.; Olson, A. J. AutoDock4 and AutoDockTools4: Automated Docking with Selective Receptor Flexibility. *J. Comput. Chem.* **2009,** *30*, 2785-2791.

53. Trott, O.; Olson, A. J. AutoDock Vina: Improving the Speed and Accuracy of Docking with a New Scoring Function, Efficient Optimization, and Multithreading. *J. Comput. Chem.* **2010,** *31*, 455-461.

54. Wang, J.; Wang, W.; Kollman, P. A.; Case, D. A. Automatic Atom Type and Bond Type Perception in Molecular Mechanical Calculations. *J. Mol. Graphics Modell.* **2006,** *25*, 247-260.

55. Case, D.; Babin, V.; Berryman, J.; Betz, R.; Cai, Q.; Cerutti, D.; Cheatham III, T.; Darden, T.; Duke, R.; Gohlke, H. Amber 14. **2014**.

56. Wang, J.; Wolf, R. M.; Caldwell, J. W.; Kollman, P. A.; Case, D. A. Development and Testing of a General Amber Force Field. *J. Comput. Chem.* **2004,** *25*, 1157-1174.

57. Maier, J. A.; Martinez, C.; Kasavajhala, K.; Wickstrom, L.; Hauser, K. E.; Simmerling, C. ff14SB: Improving the Accuracy of Protein Side Chain and Backbone Parameters from ff99SB. *J. Chem. Theory Comput.* **2015,** *11*, 3696-3713.

58. Baell, J. B.; Holloway, G. A. New Substructure Filters for Removal of Pain Assay Interference Compounds (PAINS) from Screening Libraries and for Their Exclusion in Bioassays. *J. Med. Chem.* **2010**, *53*, 2719-2740.

Table of Contents graphic